

# **Indirect assimilation of radar reflectivity with WRFDA-3DVAR and its impact on the prediction of a squall line**

Hongli Wang, Juanzhen Sun, Xiang-Yu Huang and Thomas Auligné

National Center for Atmospheric Research, Boulder, Colorado, USA

## **ABSTRACT**

An indirect radar reflectivity assimilation scheme was developed in the framework of the Weather Research and Forecast model (WRF) three-dimensional data assimilation system (WRFDA-3DVAR). The retrieved rainwater and water vapor derived from radar reflectivity were assimilated into WRFDA-3DVAR. The corresponding observation operators for rainwater and saturated water vapor were developed and incorporated into WRFDA-3DVAR. The moisture and cloud condensate control variables were pseudo relative water vapor mixing ratio and rainwater mixing ratio. A squall line case occurred on 13 June 2002 was used to assess the indirect assimilation scheme. For this case, the assimilation of reflectivity data improved short-term precipitation forecasts up to 6 hours. The assimilation of reflectivity data increased the moisture and rainwater in the cloud, and improved the forecasts of the location and intensity of the convective system.

## 1. Introduction

The radar reflectivity observations have been extensively used to provide the analysis for high-resolution numerical forecast by cloud analysis (e.g. Albers et al. 1996 ; Hu et al. 2006) or data assimilation techniques (e.g. Xiao et al. 2007; Aksoy et al. 2009). The radar data assimilation capability with Weather Research and Forecast (WRF) model three-dimensional variational data assimilation system (WRFDA-3DVAR) has been developed and evaluated in the National Center for Atmospheric Research (NCAR). To assimilate the radar reflectivity, WRFDA-3DVAR takes the approach to use total water as the moisture control variable and a partition scheme to split it into water vapor, cloud water and rainwater. The scheme and its performance evaluation were reported by Xiao et al. (2007a-b). The results from an IHOP case of 12-13 June 2002 showed that quantitative precipitation forecast (QPF) was improved over the experiments without radar data assimilation.

Though the positive results have been reported, this approach does not work well when a “dry” background is used because of the use of a linear  $Z-q_r$  equation as observation operator and the warm rain partition scheme (Sugimoto et al. 2009). The “dry” background means there is no or almost no rainwater in the background whereas reflectivity from hydrometeors exists. It occurs when WRFDA-3DVAR uses a first guess that has location errors in precipitation forecast, or is initiated from a coarse resolution analysis. In this case, the linear  $Z-q_r$  equation is either not valid (the background rainwater is zero) or produces the larger gradient to rainwater which may result in a difficult convergence of the cost function. To make the warm rain partition scheme works well, a first guess is requested which can turn on the “on-off” switches in the warm rain process. So in some studies using WRFDA-3DVAR, physical initialization (Yang et al. 2006) or cloud analysis procedures (Sugimoto et al., 2009) were carried out before the radar reflectivity assimilation. In addition, as note by Xiao et al. (2007a), the addition of the ice phase in the hydrometeor partitioning scheme was needed to broaden its application into winter season storms in which cold rain process may play an important role.

Radar reflectivity observation has been applied in cloud analysis schemes to adjust

the atmosphere variables, such as water vapor and cloud condensates (e.g. Albers et al. 1996; Hu et al. 2006; Sugimoto et al. 2009), or to derive water vapor or relative humidity (Sokol et al. 2009; Caumont et al. 2010; Ikuta et al. 2011), which is then assimilated. Some researchers (e.g. Yang et al. 2006; Sugimoto, et al., 2009) replaced the background humidity by (nearly) saturated moisture directly. It is a reasonable assumption that humidity in cloud is saturated where the reflectivity is large than a threshold. We take this assumption to produce the pseudo saturated water vapor observation.

In this study, we apply this assumption to produce the pseudo-saturated water vapor and use it in the cost function as an observation. Instead of using the water vapor information in physical initialization or cloud analysis schemes (e.g. Albers et al. 1996; Hu et al. 2006; Yang et al. 2006; Sugimoto, et al., 2009), it is used in a variational data assimilation scheme to optimally adjust the first guess toward the derived water vapor. The assimilation of the water vapor provides a favorable environment that supports the convection. In addition, the retrieved rainwater, which can be obtained by the Z-q<sub>r</sub> equation (Sun et al. 1997), is assimilated. The assimilation of the retrieved rainwater doesn't require a wet background, and also give a good rainwater analysis (Wang et al. 2011). We call this scheme as the indirect approach for radar reflectivity assimilation. The scheme is developed within WRFDA-3DVAR, and tested with a convection case. The next section describes the method. The results are shown in Section 3. A summary is in the final section.

## **2. Method**

### **2.1. WRFDA-3DVAR**

The WRFDA-3DVAR adopts the incremental VAR formulation that is commonly used in operational systems. The incremental approach is designed to find the analysis increment that minimizes a cost function defined as a function of the analysis increment by using a linearized observation operator.

$$J(\mathbf{v}) = J^b + J^o$$

$$= \frac{1}{2} \mathbf{v}^T \mathbf{v} + \frac{1}{2} (\mathbf{d} - \mathbf{H}' \mathbf{U} \mathbf{v})^T R^{-1} (\mathbf{d} - \mathbf{H}' \mathbf{U} \mathbf{v}) \quad (1)$$

where  $\mathbf{d} = \mathbf{y}^o - H(\mathbf{x}_b)$  is the innovation vector and  $\mathbf{H}'$  is the linearization of the observation operator  $H$  used in the calculation of  $\mathbf{d}$ .

## 2.2. Assimilating retrieved rainwater

The retrieved rainwater is derived from the nonlinear  $Z$ - $q_r$  relation (Sun and Crook, 1997):

$$Z = c_1 + c_2 \bullet \log_{10}(r \bullet q_r) \quad (2)$$

Since the rainwater is the analysis variable, the observation operator used here is the standard bilinear interpolation function in WRFDA-3DVAR.

## 2.3. Assimilating derived water vapor

We assume that the relative humidity in cloud is 100% where radar reflectivity is higher than a threshold, so the water vapor observation equals the saturated water vapor in the background. In this paper the threshold is set to 30 dBZ. The error of water vapor observation is specified by the relative humidity error with a reduced value of 20%. The relation between rainwater and relative humidity in cloud (hereafter  $q_r - rh$  relation) is examined by WRF model output in Section 3.4.

The observation operator  $H$  is,

$$q_v = rh \cdot q_s \quad (3)$$

where  $q_v$  and  $q_s$  stand for specific humidity and saturated specific humidity of water vapor, respectively.

The linear observation operator  $\mathbf{H}'$  is:

$$dq_v = drh \cdot q_s + rh \cdot dq_s \quad (4)$$

where

$$q_s = \frac{e e_s}{p - (1 - e) e_s} \quad (5)$$

$$e_s = c_1 \exp\left(\frac{c_2 T}{T + c_3}\right) \quad (6)$$

$$c_1=6.112, \quad c_2=17.67, \text{ and } c_3=243.5$$

Using equation (5)-(6), equation (4) can be written as

$$dq_v = q_s \cdot drh + rh \cdot \left( \frac{\partial q_s}{\partial p} \cdot dp + \frac{\partial q_s}{\partial e_s} \cdot \frac{\partial e_s}{\partial T} dT \right) \quad (7)$$

It is physically reasonable that the perturbation in humidity affects pressure and temperature in conditions that moisture is close to saturation (Bannister, 2008).

We assume the perturbation in pressure is caused by the perturbation in temperature through state equation,

$$p = rRT \quad (8)$$

The final linearized observation operator **H'** is simplified as,

$$dq_v \approx q_s \cdot drh + q_v \cdot \left( \frac{c_2 c_3}{(T + c_3)^2} - \frac{e}{T} \right) \cdot dT \quad (9)$$

### 3. IHOP case and experiment configuration

#### 3.1. IHOP case

A squall line that occurred in Oklahoma and Kansas on 12–13 June 2002 during IHOP\_2002 field experiment is chosen for this study. This study focuses on a northeast-to-southwest-oriented squall line from the Kansas and Oklahoma border to the Texas Panhandle, initiated at around 2100 UTC 12 June 2002. Isolated convective cells formed from the Kansas and Oklahoma border to the Texas Panhandle along a dryline at 2100 UTC 12 June. At 0000 UTC 13 June, a squall-line structure was well developed in the reflectivity field, with the intense convection in a triple-point area near the Kansas and Oklahoma border. It then moved southeastward and dissipated after 0900 UTC 13 June 2002.

### ***3.2 Forecast model***

The WRF-ARW model is used as the forecast model (Skamarock et al. 2008). The WRF is the next generation mesoscale model designed to serve both operational forecasting and atmospheric research applications. The model uses a third order Runge-Kutta time integration, third to fifth order advection operators, and split-explicit fast wave integration conserving both mass and energy. The model physics options include the rapid radiative transfer model (RRTM) longwave radiation, Dudhia shortwave radiation, Yonsei University (YSU) PBL schemes, and Thompson microphysics in all the experiments.

### ***3.3 Background error***

In this study, the preconditioned control variables are streamfunction, the unbalanced components of velocity potential, temperature, surface pressure, pseudo relative humidity and rainwater mixing ratio. The background error covariance matrix is estimated in the 13 June 2002 IHOP case using the ensemble method. A 20-member ensemble of convection-resolving simulations is initiated at 1200 UTC on 12 June 2002 at 4 km resolution. The 12 h forecasts at 0000 UTC 13 June 2002 are used to obtain the statistics. The length scale of the first Empirical Orthogonal Function (EOF) mode of the control variables (streamfunction, the unbalanced components of velocity potential, temperature, pseudo relative humidity and rainwater mixing ratio) is, 115.6, 90.8, 16.5, 36.6 and 7.7 km, respectively. For the rainwater the first 7 EOFs account for 99% of the total variance.

### ***3.4 Observations***

The method of Doppler radar data quality control and other preprocessing procedures are the same as that described in Xiao et al. (2007a-b). The surface observations from IHOP\_2002 field experiment are used. The assumed the  $q_r - rh$  relation in cloud is examined by the ensemble forecasts that are used to generate the

background error statistics at 0000 UTC June 2002 in section 3.3. It is found that the relative humidity is generally greater than 95%. An example of the  $q_r - rh$  relation from the output of the first ensemble is shown in figure 1.

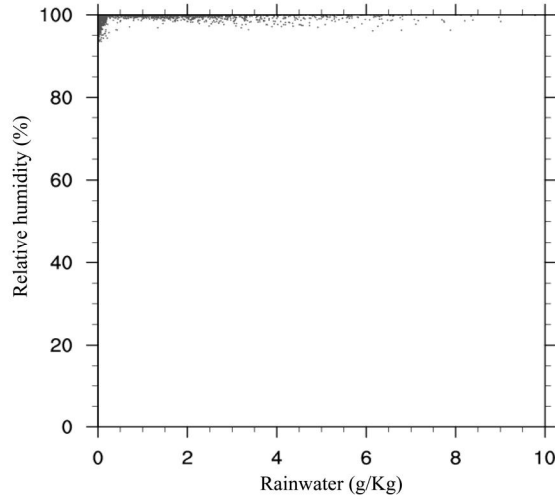


Figure 1. The example of  $q_r - rh$  relation from the model forecast.

### 3.5 Experiment

Table 1. Experiments and descriptions

Experiment	Description
CON	No data assimilation
CRV	Conventional observation with radial velocity
ALL	Conventional observation with radial velocity and reflectivity

Three numerical experiments (Table. 1) are conducted to examine the impact of radar observations on analysis and precipitation forecast. The control experiment (CON) is the 9 hour WRF simulation with initial and boundary conditions interpolated from Eta model 40 km analysis at 2100 UTC 12 June 2002. For the data assimilation experiments (CRV and ALL), the starting time is 0000 UTC 13 June 2002. The 3 hour forecast in the experiment CON is used as the first guess in the data assimilation experiments. In the experiments CRV and ALL, we only assimilate the radial velocity in the rain region defined by the reflectivity values larger than or equal

to 15 dBZ.

## 4. Results

### 4.1. Single reflectivity observation test

Before conducting the real data experiments, a single observation data assimilation test is carried out to estimate the spread of the observation by the background error statistics. The single reflectivity observation test uses 3 hour forecast at 0000 UTC 13 June 2002 as the first guess, and the assimilated reflectivity is at (34.314°N, 124.003°E; 11<sup>th</sup> model level). The innovation of the single reflectivity was assigned 10 dBZ, which is converted to rainwater about 3.0 g/kg.

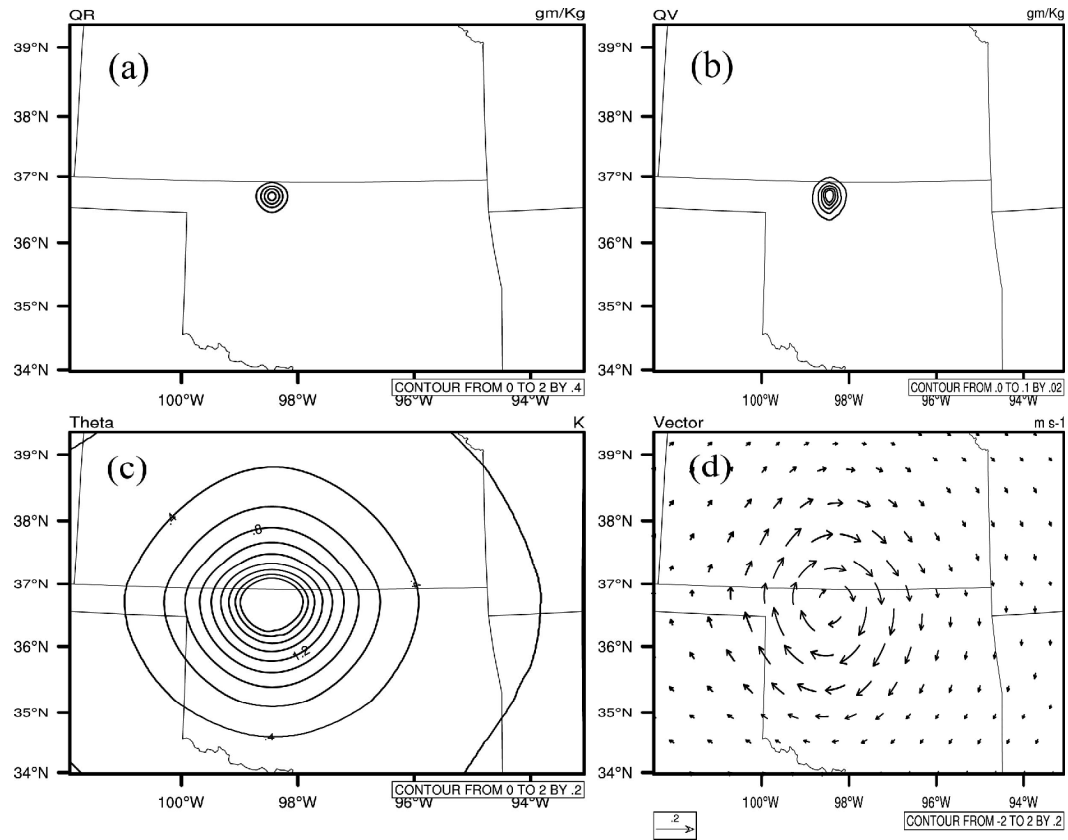


Figure 2. Increment of (a) rainwater, (b) water vapor, (c) potential temperature, and (d) wind vector. The incremental of wind and potential temperature is scaled by 1000.0.

Figure 2 shows the 3DVAR analysis increment responses at 11<sup>th</sup> model level. First of all, the rainwater mixing ratio and water vapor mixing ratio have positive analysis increments centered at the observation location (Figure 2a-b). The positive increment



arises because the two variables are underpredicted in the background. The water vapor spreads broader than the rainwater since the length scale of the water vapor is larger than the rainwater. The impact of temperature perturbation is considered in the observation operator for water vapor assimilation, so that a weak positive potential temperature increment is also found (Figure 2c). Through the wind and temperature statistical relation in the background covariance, the wind response is obtained (Figure 2d). To summarize, in the indirect assimilation scheme, a single reflectivity observation will produce the multivariate analysis.

## ***4.2. The IHOP case***

### ***4.2.1 Hourly precipitation prediction***

We first examine the impact of radar data assimilation on the hourly precipitation prediction. Figure 3 shows the stage IV precipitation observations and hourly precipitation forecasts from the two data assimilation experiments at the forecast hours of 2, 4, and 6. Among the three experiments, the experiment ALL (Figure 3j-l) is closest to the observed precipitation (Figure 3a-c). Both the experiments CON (Figure 3d-e) and CRV (Figure 3g-i) produce simulations that move too fast to the south for the precipitation band over the north Oklahoma. This location error exists in the background and is not corrected by assimilating the radial velocity alone. The simulations in CON and CRV also show more scattered precipitations rather than the banded convection as in the observations. In the experiment ALL, the assimilation of conventional data along with radial velocity and reflectivity give the best precipitation location and intensity forecast (Figure 3j-l) of the major convective band, suggesting that the indirect reflectivity assimilation method is effective to correct the location error in the background field.

Figure 4 shows The Equitable Threat Score (ETS) of the three experiments between the hourly forecast precipitation and the observed. Consistent with Figure 3, the experiment ALL improves the ETS up to 6 hours. RV has a positive impact in first 4 hours for the ETS at threshold 1.0- and 5.0 mm. For both CRV and ALL, the ETS

decreases in the second hour which seems to indicate there is a spin up adjustment in the first 2 hours

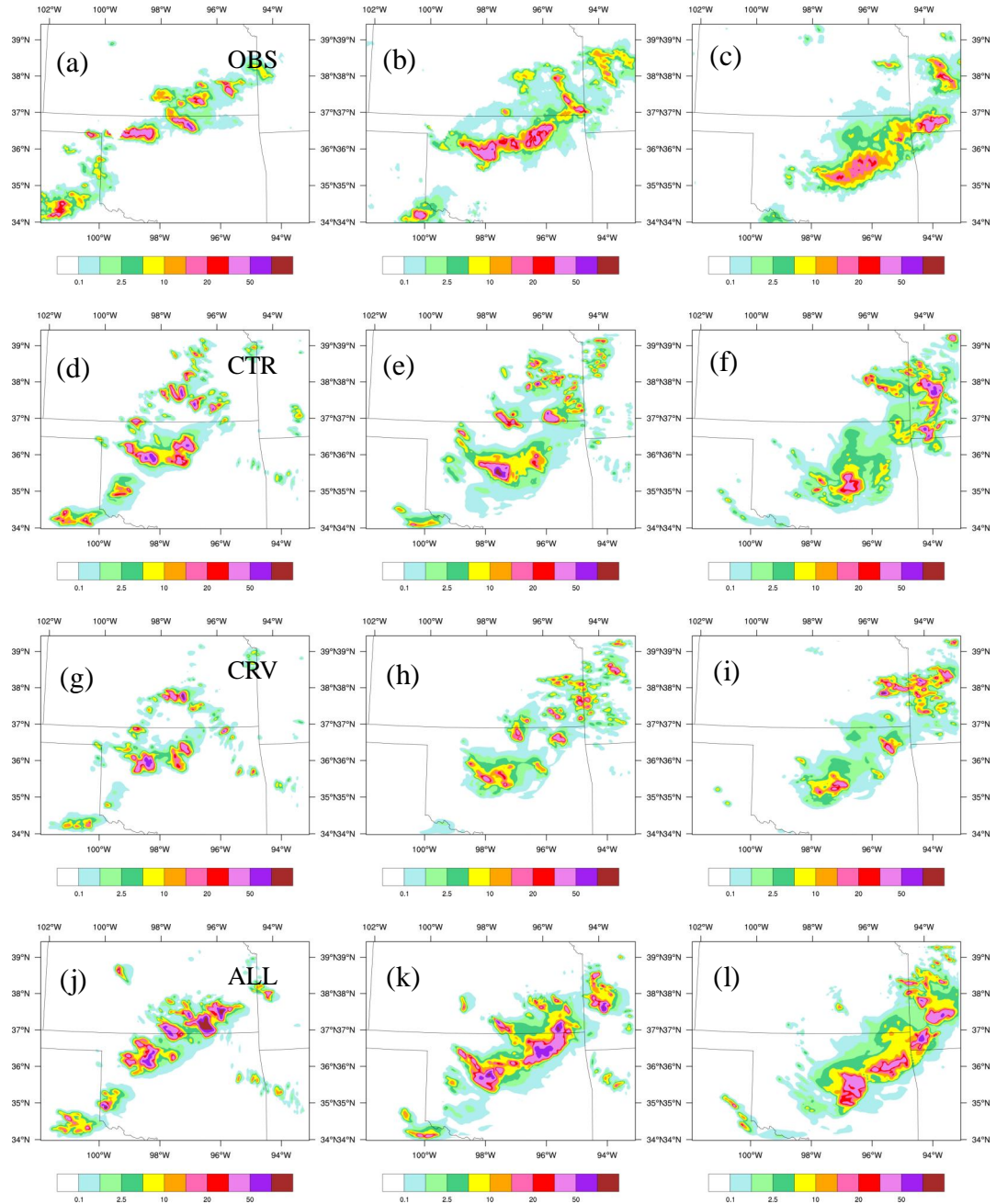


Figure 3. Hourly accumulated precipitation. (a)-(c) Stage IV observation, (d)-(f) CON, (g)-(i) CRV, (j)-(l) ALL. The left column is at 0200 UTC 13 June, the median column is at 0400 UTC 13 June, and the right column is at 0600 UCT 13 June 2002.

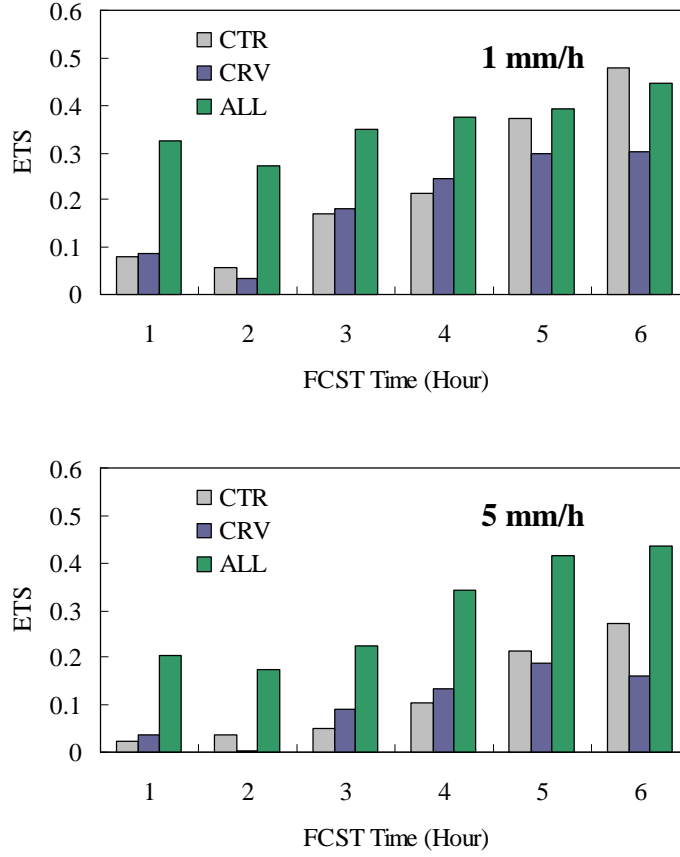


Figure 4. ETS of three experiments at threshold of 1.0 mm and 5.0 mm.

#### 4.2.2 The analysis increments

Figure 5 shows the increments of the experiment ALL. From Fig. 5a, it is found that assimilation of RV produces a convergence line in the analysis increment, which is helpful for the maintenance of the convection. The wind increment results in potential temperature increment (Fig. 5b) through the wind-temperature balance relation in the background covariance. As noted before, the forecasted convection in the first guess has a southward location bias at the assimilation time. The correction of the location error is clearly shown in the rainwater increment (Fig 4d). In the analysis produced by the experiment ALL, the water vapor and rainwater analysis is more consistent with the wind analysis, thus have large impact on the forecast.

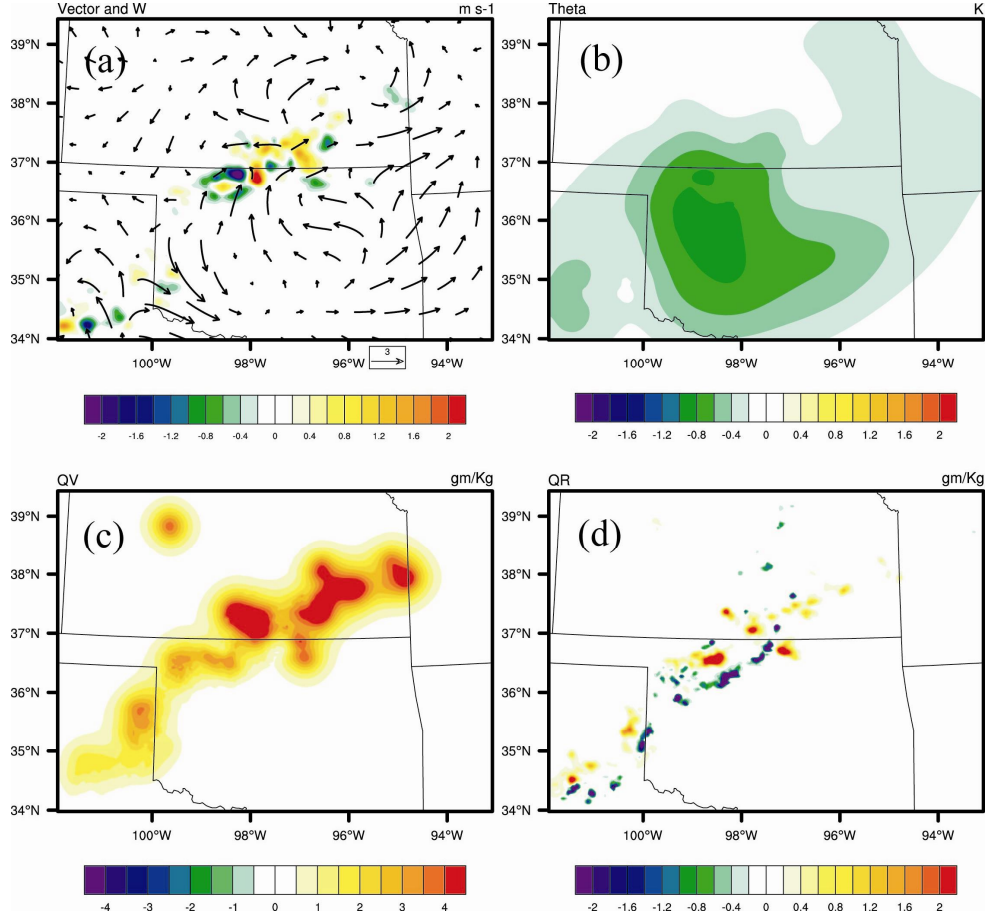


Figure 5. Increment of the experiment ALL. (a) wind vector and vertical velocity, (b) potential temperature, (c) water vapor, and (d) rainwater

## 5. Summary

The radar data assimilation capability with WRFDA-3DVAR has been developed and evaluated by Xiao et al. (2007a). To assimilate the radar reflectivity, WRFDA-3DVAR takes the approach to use total water as the moisture control variable and a partition scheme to split it into water vapor, cloud water and rainwater. The results from an IHOP case of 12-13 June 2002 showed that quantitative precipitation forecast was improved over the experiments without radar data assimilation (Xiao et al. 2007b). Though the positive results have been reported, this approach does not work well when a “dry” background is used because of the use of the linear  $Z-q_r$  equation as observation operator and the warm-rain partition scheme (Sugimoto et al. 2009).

In this study, an indirect radar reflectivity assimilation scheme was developed

within WRFDA-3DVAR system. The retrieved rainwater and water vapor derived from radar reflectivity were assimilated into WRFDA-3DVAR. The corresponding observation operators for rainwater and saturated water vapor were developed and incorporated into WRFDA-3DVAR. The moisture and cloud condensate control variables were pseudo relative water vapor mixing ratio and rainwater mixing ratio. Before conducting the real data experiments, a single observation data assimilation test was carried out to estimate the spread of the observation by the background error statistics. The results indicated that in the indirect assimilation scheme, a single reflectivity observation produced the multivariate analysis. A convection case occurred on 13 June 2002 was used to assess the indirect assimilation scheme. For this case, the assimilation of reflectivity data improved short-term precipitation forecasts up to 6 hours. The assimilation of reflectivity data increased the moisture and temperature in the cloud, and improved the forecasts of the location and intensity of the convective system.

## Reference

1. Albers, Steven C., John A. McGinley, Daniel L. Birkenheuer, John R. Smart (1996), The Local Analysis and Prediction System (LAPS): Analyses of Clouds, Precipitation, and Temperature. *Wea. Forecasting*, **11**, 273–287.
2. Aksoy, Altuğ, David C. Dowell, Chris Snyder (2009), A Multicase Comparative Assessment of the Ensemble Kalman Filter for Assimilation of Radar Observations. Part I: Storm-Scale Analyses. *Mon. Wea. Rev.*, **137**, 1805–1824.
3. Bannister, R. N. (2008), A review of forecast error covariance statistics in atmospheric variational data assimilation. II: Modelling the forecast error covariance statistics. *Quart. J. Roy. Meteor. Soc.*, **134**, 1971–1996.
4. Caumont, O., V. Ducrocq, É. Wattrelot, G. Jaubert, S. Pradier-Vabre (2010), 1D+3DVar assimilation of radar reflectivity data: A proof of concept. *Tellus A*, **62**, 173–187.
5. Hagen, M., Yuter, S.A., 2003. Relations between radar reflectivity, liquid water content, and rainfall rate during the MAP SOP. *Q. J. R. Meteorol. Soc* **129**, 477–493.
6. Hu, Ming, Ming Xue, Keith Brewster (2006), 3DVAR and Cloud Analysis with WSR-88D Level-II Data for the Prediction of the Fort Worth, Texas, Tornadoic Thunderstorms. Part I: Cloud Analysis and Its Impact. *Mon. Wea. Rev.*, **134**, 675–698.
7. Ikuta, Yasutaka and Y. Honda Indirect reflectivity assimilation approach using radar simulator in JMA non-hydrostatic model based variational data assimilation system, 91st American Meteorological Society Annual Meeting, Seattle, WA. 23-27 January 2011
8. Skamarock, W. C., Klemp, J. B., Dudhia, J., Gill, D. O., Barker, D. M., Duda, M., Huang, X. -Y., Wang, W., and Powers, J. G. (2008), A description of the advanced research WRF version 3. NCAR Tech. Note TN-475+STR, 113 pp.
9. Sokol Z. and D. Rezacova (2009), Assimilation of the radar-derived water vapour mixing ratio into the LM COSMO model with a high horizontal resolution, *Atmos. Res.* **92**, 331–342.

10. Sugimoto, Soichiro, N. Andrew Crook, Juanzhen Sun, Qingnong Xiao, Dale M. Barker, (2009), An Examination of WRF 3DVAR Radar Data Assimilation on Its Capability in Retrieving Unobserved Variables and Forecasting Precipitation through Observing System Simulation Experiments. *Mon. Wea. Rev.*, 137, 4011–4029.
11. Sun, J, N. A. Crook (1997), Dynamical and Microphysical Retrieval from Doppler Radar Observations Using a Cloud Model and Its Adjoint. Part I: Model Development and Simulated Data Experiments. *JAS*, 54(12) 1642-1661
12. Xiao, Q., Kuo, Y., Sun, J., Lee, W., Barker, D. M., Lim (2007a), An approach of doppler reflectivity data assimilation and its assessment with the inland QPF of Typhoon Rusa (2002) at landfall. *Journal of Applied Meteorology and Climatology*, **46**, doi: [10.1175/JAM2439.1](https://doi.org/10.1175/JAM2439.1), 14-22.
13. Xiao, Qingnong, Juanzhen Sun (2007b), Multiple-Radar Data Assimilation and Short-Range Quantitative Precipitation Forecasting of a Squall Line Observed during IHOP\_2002. *Mon. Wea. Rev.*, **135**, 3381–3404.
14. Yang, Y., C. Qiu, and J. Gong (2006), Physical initialization applied in WRF-Var for assimilation of Doppler radar data, *Geophys. Res. Lett.*, 33, L22807, doi:10.1029/2006GL027656.
15. Wang, H. L., J. Sun, Y. R. Guo, and X. Y. Huang (2011), Radar Reflectivity Assimilation with the updated WRFDA-4DVAR system, 91st American Meteorological Society Annual Meeting, Seattle, WA. 23-27 January 2011.